Diet is one of the most important modifiable cancer risk determinants[15]. Dietary components have been implicated in many pathways involved in carcinogenesis. In addition, carcinogenic processes are associated with the altered expression of several miRNAs. Recent studies have reported that a widespread down-regulation of miRNAs is commonly observed during human cancer-cell initiation and progression[16,17]. In this study, we hypothesised that the dietary intake of natural products maintains tumour-suppressive miRNA expression in cancer cells, leading to the prevention of carcinogenesis. We demonstrated that resveratrol suppresses cancer cell malignancy *in vitro* and *in vivo* through the transcriptional activation of tumour-suppressive miRNAs and Argonaute2 (Ago2). Furthermore, we provided evidence that Ago2 over-expression enhances the RNA interference (RNAi) activity. These findings suggest that the dietary intake of natural products safely reduces a wide range of negative consequences with an overall improvement in human health and survival by modulating miRNA biogenesis.

Results

Resveratrol reduces the cancer stem-like cells population by up-regulating miR-141 and miR-200c. To identify the potential anti-cancer activity of resveratrol, we investigated the effects of this compound on tumour formation *in vivo*. We orthotopically inoculated female SCID hairless outbred mice with MDA-MB-231-luc-D3H2LN cells (200 cells), which were then treated with resveratrol (25 mg/kg/day) or ethanol (control) via intraperitoneal injection every day for one week. Tumour growth was then monitored using an IVIS imaging system. The weight of the mice did not significantly change between the groups during the course of the experiment, suggesting that resveratrol did not have notable adverse effects on mice (Supplementary Fig. 1a). The results demonstrated that the resveratrol administration into the mice significantly suppressed tumour formation, while obvious tumours were observed in vehicle-treated mice, indicating that resveratrol is capable of inhibiting the survival and growth of cancer cells *in vivo* (Fig. 1a). A recent report has shown that solid tumours contain a distinct population of cells with the ability to form tumours in mice; these cells are known as tumour-initiating or cancer stem-like cells (CSCs) and display increased drug resistance and metastatic ability because they consistently form tumours, whereas other cancer cell populations were depleted of cells capable of tumour formation[18,19]. To identify the effects of resveratrol on the CSC phenotype, breast cancer cells were examined for changes in the CSC population, which is a highly tumourigenic $CD44^+/CD24^-$ subpopulation with stem cell-like self-renewal properties and the ability to produce differentiated progeny after resveratrol treatment[18]. Compared to vehicle-treated control cells, cells treated with 50 μM resveratrol demonstrated a significant 6-fold decrease in the $CD44^+/CD24^-$ population in MDA-MB-231-luc-D3H2LN cells (Fig. 1b). In addition, mammosphere formation, which has been widely used for breast CSC enrichment, of the $CD44^+/CD24^-$ fraction from MDA-MB-231-luc-D3H2LN cells was suppressed after resveratrol treatment (Supplementary Fig. 1b). We also assessed apoptosis using TUNEL staining and a caspase assay and found that resveratrol did not induce apoptosis (Supplementary Figs. 1c and 1d). Human breast cancers are driven by a CSC component that may contribute to tumour metastasis and therapeutic resistance[20]. Indeed, we found that the combination of resveratrol with low therapeutic doses of docetaxel elicits significantly greater cancer cell growth inhibition *in vitro* and *in vivo* (Supplementary Figs. 1e–g). These findings strongly suggest that resveratrol demonstrates multiple anti-cancer effects through the reduction of the CSC population.

To examine whether resveratrol could influence the breast cancer cell metastasis ability, the highly invasive breast cancer cell line MDA-MB-231-luc-D3H2LN was used in *in vitro* invasion assays. As shown in Fig. 1c, the invasion of MDA-MB-231-luc-D3H2LN cells was suppressed by resveratrol treatment. Previous studies have documented aberrant miRNA expression in cancer, and our observations prompted us to hypothesise that the anti-cancer resveratrol effects were mediated by miRNAs, particularly by a group of tumour-suppressive miRNAs[21]. A recent study has demonstrated that miR-141 and miR-200c strongly inhibit breast cancer invasion ability[22]. We found that resveratrol exposure increases miR-141 and miR-200c expression in MDA-MB-231-luc-D3H2LN cells (Fig. 1d). These findings suggest that resveratrol exhibits multiple anti-cancer effects through the inhibition of CSC phenotypes by activating miR-141 and miR-200c. In addition, to determine whether the up-regulation of miR-141 and miR-200c is mediated at the transcriptional level, we measured the expression levels of the primary miRNAs of miR-141 and miR-200c and found that these miRNAs are up-regulated at the primary transcript level (Supplementary Fig. 1h). Taken together, these results indicate that resveratrol increases the expression of tumour-suppressive miRNAs via the induction of miRNA transcription. Similar results were obtained in two other human breast cancer cell lines (MCF7 and MCF7-ADR) and MCF10A, an immortalised, non-transformed epithelial cell line (Supplementary Figs. 2–4).

Resveratrol up-regulates the expression of tumour-suppressive miRNAs. We demonstrated that resveratrol specifically reduced the CSC fraction (Fig. 1b). In addition, we also observed that miR-141 and miR-200c, which are known to suppress the CSC phenotype, are both induced by resveratrol treatment (Fig. 1d). These observations suggest that a part of the anti-cancer effects of resveratrol is mediated by miRNAs, particularly tumour-suppressive miRNAs. Indeed, a morphological change is observed after resveratrol treatment (Fig. 2a), suggesting that resveratrol induces a variety of miRNAs in cancer cells. To confirm whether miRNAs are globally up-regulated in the multiple anti-cancer effects induced by resveratrol in MDA-MB-231-luc-D3H2LN cells, we performed a comprehensive miRNA profiling of untreated MDA-MB-231-luc-D3H2LN cells and compared the results to those obtained in resveratrol-treated cells. As shown in Fig. 2b, we found that a subset of tumour-suppressive miRNAs is transcriptionally up-regulated by resveratrol (Table 1). To validate the microarray results, we performed qRT-PCR. A set of mature tumour-suppressive miRNAs, including miR-16 and miR-143, are significantly up-regulated in a variety of breast cancer cell lines, including MDA-MB-231-luc-D3H2LN, MCF7, MCF7-ADR, and MCF10A (Supplementary Figs. 2–5). These results indicated that resveratrol globally up-regulates tumour-suppressive miRNAs in human breast normal epithelial and cancer cells.

Resveratrol enhances the Ago2 RNAi potency. Although our data provide evidence that resveratrol globally up-regulates tumour-suppressive miRNAs and one of the mechanisms that is mediated by primary miRNA up-regulation, we also hypothesised that changes at other levels of the RNAi pathway may play a role in enhancing the resveratrol-mediated miRNA activity in cells in addition to transcriptional alterations. It is known that miRNA generation occurs in a multi-step process[23,24]. If one of the components associated with the miRNA pathway is under-expressed or qualitatively impaired, the pathway as a whole is destabilised. To examine the effect of resveratrol on the miRNA machinery, we measured the expression levels of a selected group of miRNA machinery-related genes, including Dicer1, Drosha, TARBP2, DGCR8, and Ago2, after the resveratrol treatment of MDA-MB-231-luc-D3H2LN cells. We found that resveratrol exposure significantly increased Ago2 expression in MDA-MB-231-luc-D3H2LN cells (Fig. 2c and Supplementary Fig. 6a). To elucidate the resveratrol-mediated Ago2 up-regulation mechanism, we assessed the Ago2 promoter activity and the Ago2 mRNA and protein half-lives after resveratrol treatment. As shown in supplementary Fig. 6b, the Ago2 protein half-lives were unchanged after resveratrol treatment. In contrast, the Ago2 mRNA was slightly

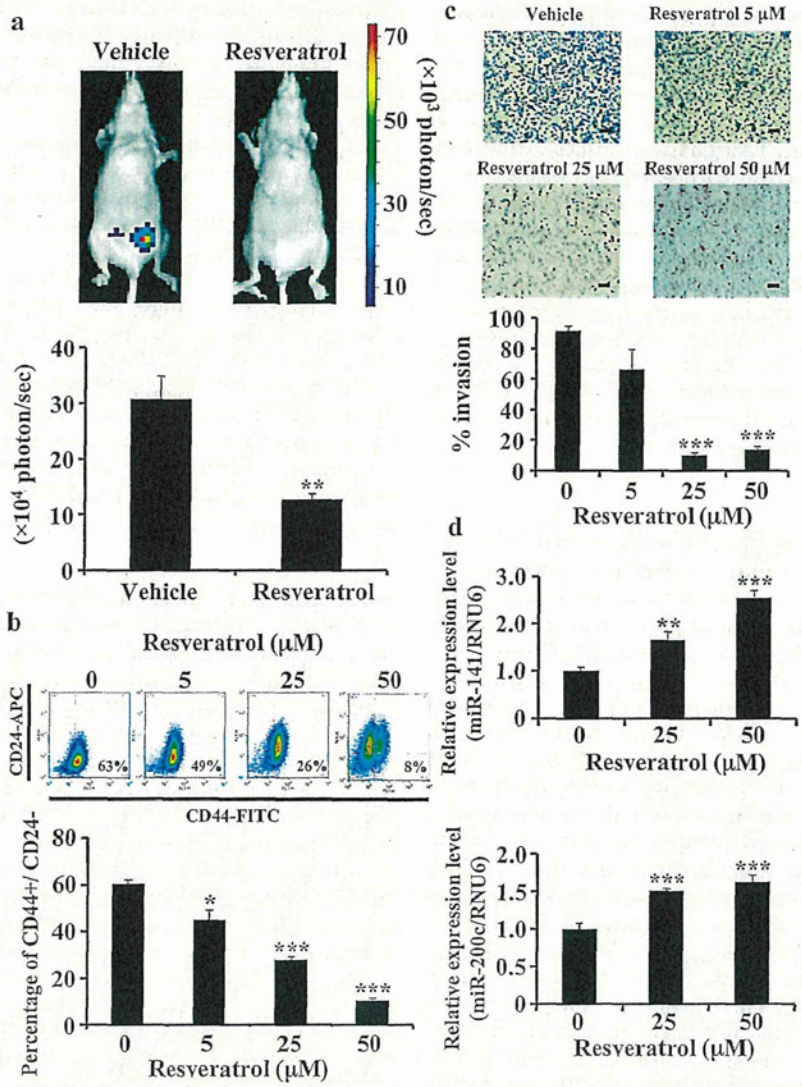

Figure 1 | Multiple anti-cancer effects of resveratrol through the activation of miR-141 and miR-200c. (a) MDA-MB231-luc-D3H2LN cells (200 cells) were injected into the mammary fat pad of six-week-old female SCID hairless outbred mice (n = 5). They were then treated with resveratrol (25 mg/kg/day) by intraperitoneal injection every day for 8 days. Tumour growth was monitored by injecting luciferin in the mice followed by measuring bioluminescence using an IVIS imaging system. Representative mouse images at day 8 (upper panel) and quantified bioluminescence images at day 8 (lower panel) are shown. (b) MDA-MB231-luc-D3H2LN cells were treated with resveratrol or DMSO (control) at the specified doses for 3 days. The percentage of $CD44^+/CD24^-$ cells after compound treatment in independent experiments with MDA-MB231-luc-D3H2LN cell populations is shown. The $CD44^+/CD24^-$ denoting the CSC-enriched fraction. (c) MDA-MB231-luc-D3H2LN cells were grown, treated with resveratrol or DMSO (control) for 1 day, and then subjected to an invasion assay. Representative photographs (upper panel) and quantification (lower panel) are shown. Scale bar: 100 μm. (d) The miR-141 and miR-200c expression levels in MDA-MB231-luc-D3H2LN cells. The expression levels of the indicated miRNAs were examined in MDA-MB231-luc-D3H2LN cells after 48 hour resveratrol treatment (all data are shown as the mean ± s.e.m., *P<0.05, **P<0.01, ***P<0.001).

increased after resveratrol treatment (Supplementary Fig. 6c). In addition, resveratrol induced the luciferase activity of a plasmid containing the Ago2 promoter upstream of the luciferase gene, suggesting that resveratrol transcriptionally induced the expression of Ago2 (Supplementary Fig. 6d). The Ago2 protein is a key regulator of miRNA homeostasis and, upon recognition, it can either cleave or remain tethered to an mRNA to repress its translation and/or regulate its stability[25]. To reveal the relationship between Ago2 and miRNAs, we first quantified the miRNA expression in MDA-MB-231-luc-D3H2LN cells transfected with the Ago2 expression vector. The induction of Ago2 expression by the Ago2 expression vector was confirmed by qRT-PCR (Fig. 2d). After transfection of the Ago2 expression vector, a subset of miRNAs including miR-16, miR-141, miR-143, and miR-200c was higher than in the control cells (Fig. 2e and Supplementary Fig. 6e). To further study the relationship between resveratrol-induced Ago2 and RNAi activity, MDA-MB-231-luc-D3H2LN cells were transfected with luciferase siRNA in the presence of resveratrol treatment and subjected to an *in vitro* firefly luciferase assay. If the induction of Ago2 expression leads to the enhancement of RNAi activity in cells, the luciferase siRNA silencing effect of the luciferase gene in MDA-MB-231-luc-D3H2LN cells may be enhanced after Ago2 over-expression even in the presence of a low siRNA dose and a prolonged period after siRNA transfection. As shown in Fig. 2f, the resveratrol-induced Ago2 resulted in a long-term gene-silencing response in MDA-MB-231-luc-D3H2LN cells. In addition, Ago2 over-expression in HEK293 cells demonstrated a long-term gene-silencing response that was similar to resveratrol-treated MDA-MB-231-luc-D3H2LN cells (Supplementary Fig. 6f).

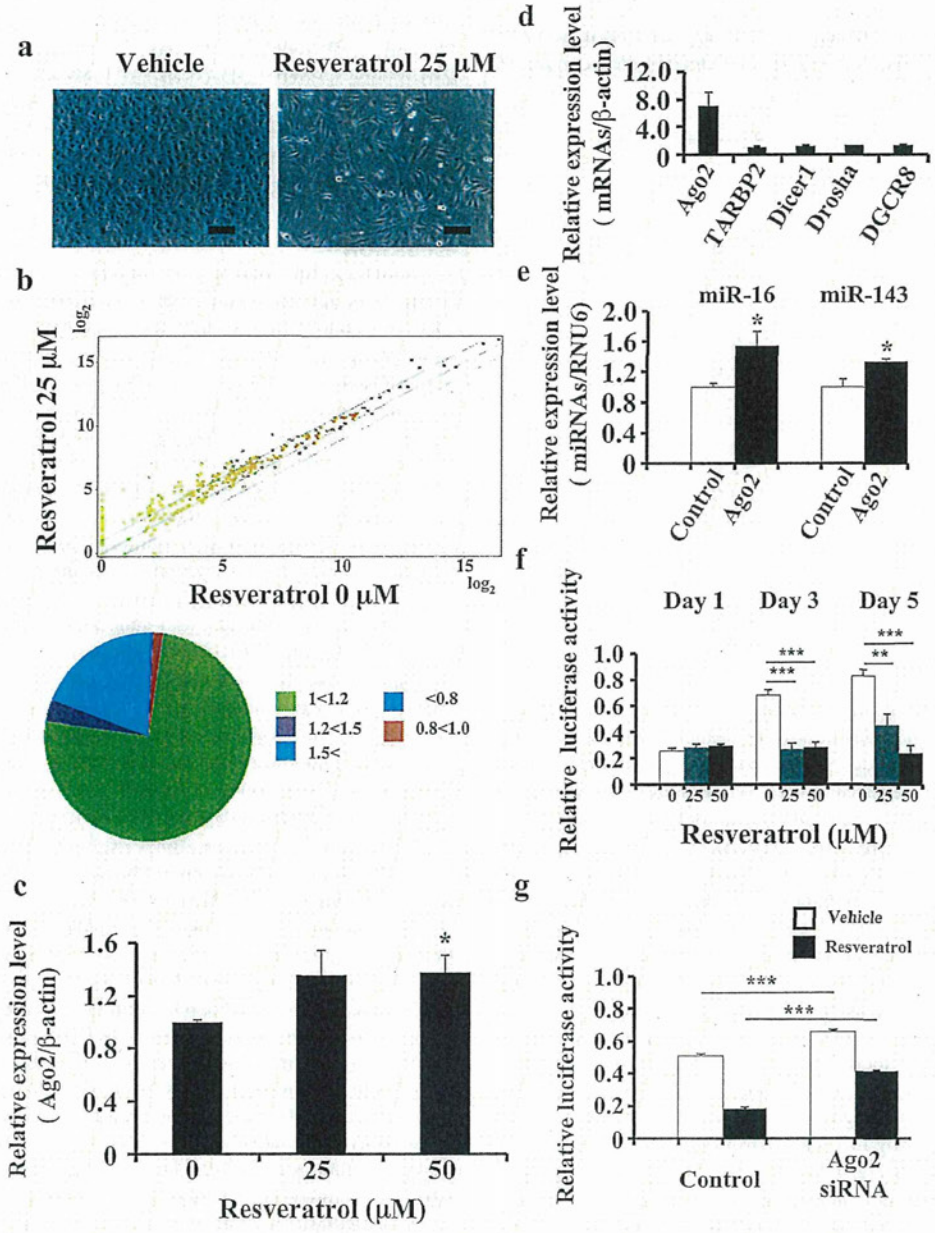

Figure 2 | Association between resveratrol and Ago2. (a) Characteristic microscopic images of MDA-MB231-luc-D3H2LN cells in the presence of DMSO (control) or resveratrol. Scale bar: 100 μm. (b) The effects of resveratrol treatment on miRNA expression in MDA-MB231-luc-D3H2LN cells by miRNA microarray analysis. The proportions of miRNAs at different fold change levels are shown in the lower panel. (c) MDA-MB231-luc-D3H2LN cells were treated with resveratrol or DMSO (control). After 2 days of culture, the cell extract was subjected to real-time mRNA qRT-PCR. (d), (e) MDA-MB231-luc-D3H2LN cells were grown and transiently transfected with Ago2 or EGFP-IRES vector (control). After 2 days of culture, the cell extract was subjected to real-time mRNA (d) and miRNA (e) qRT-PCR. The values on the *y-axis* are depicted relative to the expression level of the EGFP-IRES control vector, which is defined as 1. (f) MDA-MB231-luc-D3H2LN cells were grown and transiently transfected with luciferase siRNA or AllStars negative control siRNA (0.1 nM) under resveratrol treatment. After 1, 3, or 5 days of culture, the cells were subjected to a luciferase reporter assay. The values on the *y-axis* are depicted relative to the luciferase activity of the AllStars Negative Control siRNA, which is defined as 1. (g) MDA-MB231-luc-D3H2LN cells were grown and transiently transfected with luciferase siRNA or AllStars Negative Control siRNA and Ago2 siRNA or AllStars Negative Control siRNA. After 3 days of culture, the cells were subjected to a luciferase reporter assay. The values on the *y-axis* are depicted relative to the luciferase activity of the negative control siRNA, which is defined as 1 (all data are shown as the mean ± s.e.m., *P<0.05, **P<0.01, ***P<0.001).

Moreover, we performed an RNAi experiment to target Ago2 after resveratrol treatment and then assessed the RNAi activity demonstrated by the luciferase siRNA directed against the luciferase gene. The reduction in Ago2 expression by Ago2 siRNA was confirmed by qRT-PCR (Supplementary Fig. 6g). As shown in Fig. 2g, Ago2 siRNA-mediated silencing inhibited the RNAi activity in MDA-MB-231-luc-D3H2LN cells. Taken together, these results indicate that the resveratrol anti-cancer activities were mediated by not only tumour suppressive miRNA upregulation but also by the enhancement of the RNAi activity regulated by Ago2.

Resveratrol-induced miRNA exert an anti-cancer effect. It has been reported that miR-141 inhibits the epithelial-mesenchymal transition and cancer cell migration in breast cancer cells[26]. In addition, we found that resveratrol induced the expression of miR-141 and miR-200c in MDA-MB-231-luc-D3H2LN cells (Fig. 1d). In

Table 1 | A list of miRNAs which were up-regulated more than 2.0-fold by resveratrol in MDA-MB-231-luc-D3H2LN cells compared with control

miRNA	Fold change
Tumor-suppressive miRNA	
hsa-miR-141	4.48
hsa-miR-26a	2.33
hsa-miR-195	3.38
hsa-miR-126	2.41
hsa-miR-185	2.75
hsa-miR-340	11.07
hsa-miR-128	2.13
hsa-miR-34a	2.65
hsa-miR-193b	2.58
hsa-miR-335	2.42
hsa-miR-200c	3.47
hsa-miR-196a	2.67
hsa-miR-497	4.60
hsa-miR-125a-3p	3.00
Onco- miRNA	
hsa-miR-378*	4.81
hsa-miR-10b	5.11
hsa-miR-132	7.23
hsa-miR-222	2.40

contrast, the CSC population was decreased (Fig. 1b). To show direct evidence of whether multiple phenotypes induced by resveratrol were regulated by tumour-suppressive miRNAs, MDA-MB-231-luc-D3H2LN cells were transfected with an antisense oligonucleotide targeting miR-141 (i.e., a miR-141 inhibitor) in the presence of resveratrol treatment. MiR-141 repression by the miR-141 inhibitor was confirmed by qRT-PCR (supplementary Fig. 7a). As shown in Fig. 3a, the miR-141-induced inhibition of invasion was abrogated by the addition of the miR-141 inhibitor, and the MDA-MB-231-luc-D3H2LN cell invasiveness was increased. To confirm the link between resveratrol and miRNA expression, we investigated the growth of breast cancer cells in the presence or absence of a miR-143 inhibitor[27]. In the presence of resveratrol, miR-143-induced inhibition significantly increased the survival of MDA-MB-231-luc-D3H2LN cells relative to the control (Fig. 3b). It has been shown that miR-200c up-regulation in breast cancer cells inhibits Zeb1 expression, resulting in E-cadherin induction in breast cancer cell lines[28]. As shown in Fig. 1d, we found miR-200c up-regulation after resveratrol treatment, suggesting that resveratrol treatment activates this pathway and demonstrating its anti-cancer activity. Indeed, resveratrol addition significantly suppressed Zeb1 expression in the breast cancer cell lines (Fig. 3c) and induced E-cadherin expression in those cells (supplementary Fig. 7b). Furthermore, to show the direct effects of resveratrol on the miRNA machinery, we performed a Zeb1 3′UTR assay and demonstrated that resveratrol treatment significantly down-regulated the luciferase activity of a plasmid containing the Zeb1 3′UTR (Fig. 3d). Taken together, these results suggested that resveratrol plays an important role in breast cancer prevention by up-regulating tumour-suppressive miRNAs.

The stilbene family regulates miRNA biogenesis. The naturally occurring dimethylether resveratrol analogue pterostilbene is a stilbene family member that is generated by plants. Pterostilbene has also been reported to possess chemopreventive activity in cancer and other resveratrol-like health benefits[29,30]. To determine whether pterostilbene induced the expression of tumour-suppressive miRNAs in a similar manner as resveratrol, we assessed the effect of pterostilbene on miRNA expression. As shown in Fig. 4a, pterostilbene treatment suppressed cell growth more significantly than resveratrol treatment in MDA-MB-231-luc-D3H2LN cells. In addition, the expression of tumour suppressive miRNAs (i.e., miR-143 and miR-200c) and Ago2 was significantly higher in pterostilbene-treated MDA-MB-231-luc-D3H2LN cells than in resveratrol-treated cells (Figs. 4b-d and Supplementary Fig. 8). Taken together, these results suggest that resveratrol-induced tumour-suppressive miRNA expression and its anti-cancer activity are conserved among stilbene family members (Fig. 4e).

Discussion

Resveratrol exhibits strong anti-oxidant activity and is capable of inducing apoptosis in cancer cells. Therefore, resveratrol is believed to be efficacious at multiple carcinogenesis stages[4]. However, the underlying molecular mechanism of its anti-tumour activity has yet to be defined. In this study, we demonstrated that resveratrol up-regulated tumour-suppressive miRNAs, resulting in the induction of an anti-cancer effect against the CSC phenotype in cancer cells. We also demonstrated that resveratrol inhibited the invasiveness of breast cancer cells as one of the CSC phenotypes by activating miR-141 and miR-200c. However, the reason why resveratrol reduces the CSC population remains elusive. Recent studies have provided evidence that miR-200c strongly inhibits the ability of breast CSCs to form tumours *in vivo*[31]. These findings suggest that resveratrol shows multiple anti-cancer effects by reducing the CSC population through miR-200c activation.

Argonaute proteins are widely expressed and are involved in post-transcriptional gene silencing. Using microarrays to compare control and Ago2$^{-/-}$ cells, recent studies have demonstrated that Ago2 loss results in the global reduction of mature miRNAs in erythroblasts, fibroblasts, and hepatocytes[32]. However, it has not been determined whether Ago2 alterations can contribute to miRNA expression and the RNAi response. In this study, we show that Ago2 up-regulation by resveratrol leads to an increase in tumour-suppressive miRNAs and the enhancement of RNAi activity.

Pterostilbene has anti-diabetic properties and has been shown to be cytotoxic to a number of cancer cell lines *in vitro*[29,30]. Although pterostilbene and resveratrol have similar pharmacological properties, pterostilbene contains two methoxy groups and one hydroxyl group, while resveratrol has three hydroxyl groups (Supplementary Fig. 9). A recent study demonstrated that pterostilbene shows 95% bioavailability when orally administered, while resveratrol only has 20% bioavailability[33]. Furthermore, pterostilbene is a more powerful chemopreventive agent than resveratrol in colon cancer[34], showing that pterostilbene has several key advantages over resveratrol. In this study, we demonstrate that pterostilbene is more reliable than resveratrol in mediating the anti-cancer effect by inducing tumour-suppressive miRNAs and Ago2 expression. The reason for the difference in the anti-cancer activity of pterostilbene and resveratrol in cancer cells may be due to the expressed miRNAs.

It has been demonstrated that most tumours are characterised by globally diminished miRNA expression[16,17,35]. Thus, the delivery of tumour suppressive miRNAs may allow for the therapeutic restitution of physiological regulation programs lost in cancer and other disease states. However, miRNA therapy shares many of the disadvantages of other treatment approaches including delivery limitations and instability. Therefore, novel methods are required to resolve these issues. Based on this study, we hypothesise that the down-regulation of miRNAs in cancer cells is compensated by resveratrol, which induces the derepression of tumour suppressive miRNAs. Down-regulation of oncogenic miRNAs and up-regulation of tumour-suppressive miRNAs by resveratrol in prostate cancer cells has been reported[36]; however, the connection between resveratrol and the miRNA biogenesis machinery has not been investigated in detail. In this report, we demonstrated that resveratrol leads to a reduction in malignancy by not only activating tumour-suppressive miRNA transcription (Figs. 1d and 2b) but also enhancing the RNAi activity mediated by Ago2 induction (Figs. 2d, e, f and g). Our

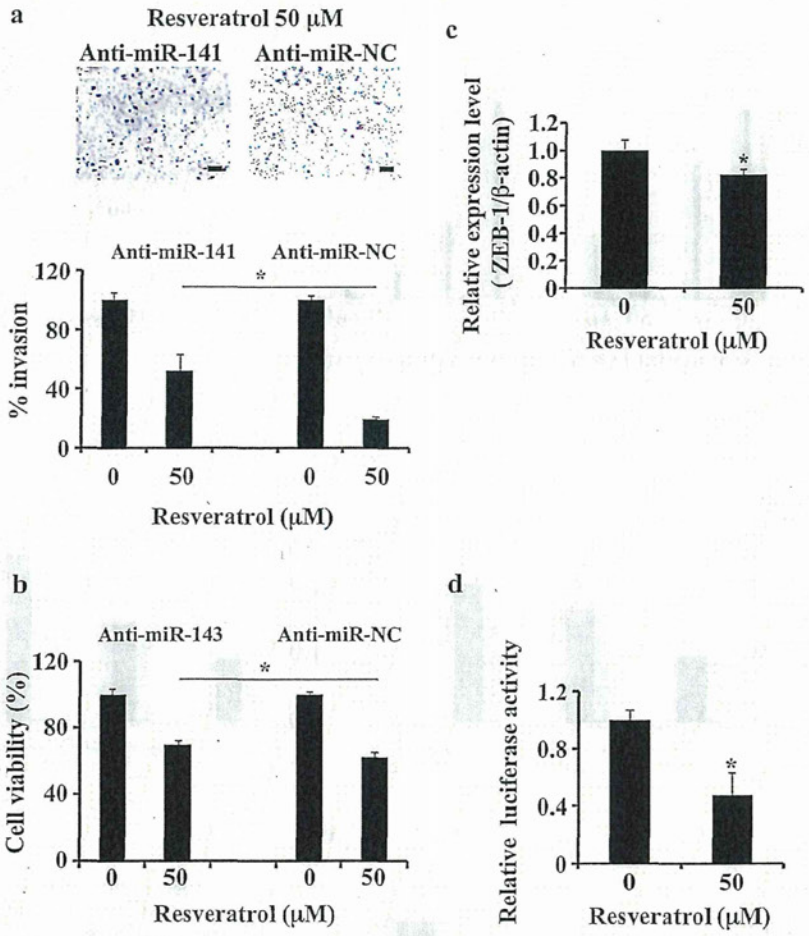

Figure 3 | Multiple anti-cancer effects of tumour-suppressive miRNAs induced by resveratrol. (a) MDA-MB231-luc-D3H2LN cells were grown and transiently transfected with anti-miR-141 or anti-miR-NC (control). After 4 hours, the cells were treated with resveratrol or DMSO (control) for 1 day and subjected to an invasion assay. Representative photographs (upper panel) and quantification (lower panel) are shown. Scale bar: 100 μm. (b) MDA-MB231-luc-D3H2LN cells were cultured and transiently transfected with anti-miR-143 or anti-miR-NC (control). After 4 hours, the cells were treated with resveratrol or DMSO (control) for 72 hours, and the cell viability was measured by the MTS assay. (c) MDA-MB231 cells were treated with resveratrol or DMSO (control). After 2 days of culture, the cell extract was subjected to real-time mRNA qRT-PCR. (d) MDA-MB231 cells were grown and transiently transfected with a ZEB-1 3′UTR or psiCheck2 vector (control) under resveratrol treatment. After 1 day of culture, the cells were subjected to a luciferase reporter assay. The values on the *y-axis* are depicted relative to the luciferase activity of cells treated with DMSO, which is defined as 1 (all data are shown as the mean ± s.e.m., *P<0.05).

demonstration that resveratrol potently suppresses even a severe and multifocal carcinogenesis model in the absence of measurable toxicity provides proof of the principle that miRNA replacement by resveratrol may be a clinically viable anti-cancer therapeutic strategy.

In conclusion, this study shows that an orally available small molecule can safely reduce many of the negative consequences at doses acceptable in humans with an overall improvement in health and survival. Our results raise the possibility that the regulation of tumour-suppressive miRNAs by natural agents could be a novel strategy in the design of combinational approaches using conventional therapies for tumour recurrence prevention and in achieving successful treatment outcomes in patients with cancer.

Methods

Reagents. Trans-resveratrol (98% purity) was purchased from Cayman Chemical, pterostilbene (98% purity) from Tokyo Chemical Industry, cycloheximide solution and 5, 6-dichlorobenzimidazole riboside from sigma, and docetaxel from Sanofi-Aventis. The antibiotic solution (containing 10,000 U/mL penicillin and 10 mg/mL streptomycin), the trypsin-EDTA mixture (containing 0.05% trypsin and EDTA), and FBS (fetal bovine serum) were obtained from Invitrogen. The FITC-conjugated anti-CD44 (clone L178) antibody was obtained from Becton Dickinson, and the APC- conjugated anti-CD24 (clone ML5) antibody, from Biolegend. The duplexes of each small interfering RNA (siRNA), targeting human Ago2 mRNA (siAgo2-1, GCACGGAAGUCCAUCUGAAUU, UUCAGAUGGACUUCCGUGCUU; siAgo2-2, GCAGGACAAAGAUGUAUUAUU, UAAUACAUCUUUGUCCUGCUU; siAgo2-3, GGGUCUGUGGUGAUAAAUAUU, UAUUUAUCACCACAGACCCUU; siAgo2-4, GUAUGAGAACCCAAUGUCAUU, UGACAUUGGGUUCUCAUACUU) and negative control 1 were purchased from Applied Biosystems[37].

Plasmids. The primary-miR-143 expression vector was purchased from TaKaRa BIO. The full-length human Ago2 cDNA was cloned into pIRES2-EGFP vector (Clontech). We amplified the upstream of human Ago2 gene (−1,770/−1 relative to the TSS) by PCR using human genomic DNA as template, and we cloned it into the pGL3-Basic vector. For the 3′UTR reporter plasmids, the nucleotides +3,399 to +3,953 of human ZEB1 cDNA were amplified and cloned downstream of the luciferase gene in the psiCHECK2 vector (Promega). For cloning the following primers were used for PCR: Ago2 promoter: 5′-ACGCGTATAGGGGATATGTGAAGGAGACA-3′ (forward) and 5′-CTCGAGATA CGCGCGCGCCACGGGCCCCG-3′ (reverse); ZEB1 3′UTR Fragment: 5′-ATAATACGCGTTAAAGGAAGCTGATTAATTAGATATGC-3′ (forward) and 5′-ATAATAAGCTTTTTGTAGTGCAGAAGTTCTCACATTTT-3′ (reverse)[22].

Cell culture. HEK293 cells (American Type Culture Collection) were cultured in Dulbecco's Modified Eagle's Medium containing 10% heat-inactivated FBS and an antibiotic-antimycotic (Invitrogen) at 37°C in 5% CO_2. MDA-MB-231 cells (American Type Culture Collection) and MDA-MB-231-luc-D3H2LN cells (Xenogen) were cultured in RPMI containing 10% heat-inactivated FBS and antibiotic-antimycotic at 37°C in 5% CO_2. Human mammary carcinoma cell lines, MCF7 cells and multidrug-resistant MCF7-ADR cells were provided by Shien-Lab,

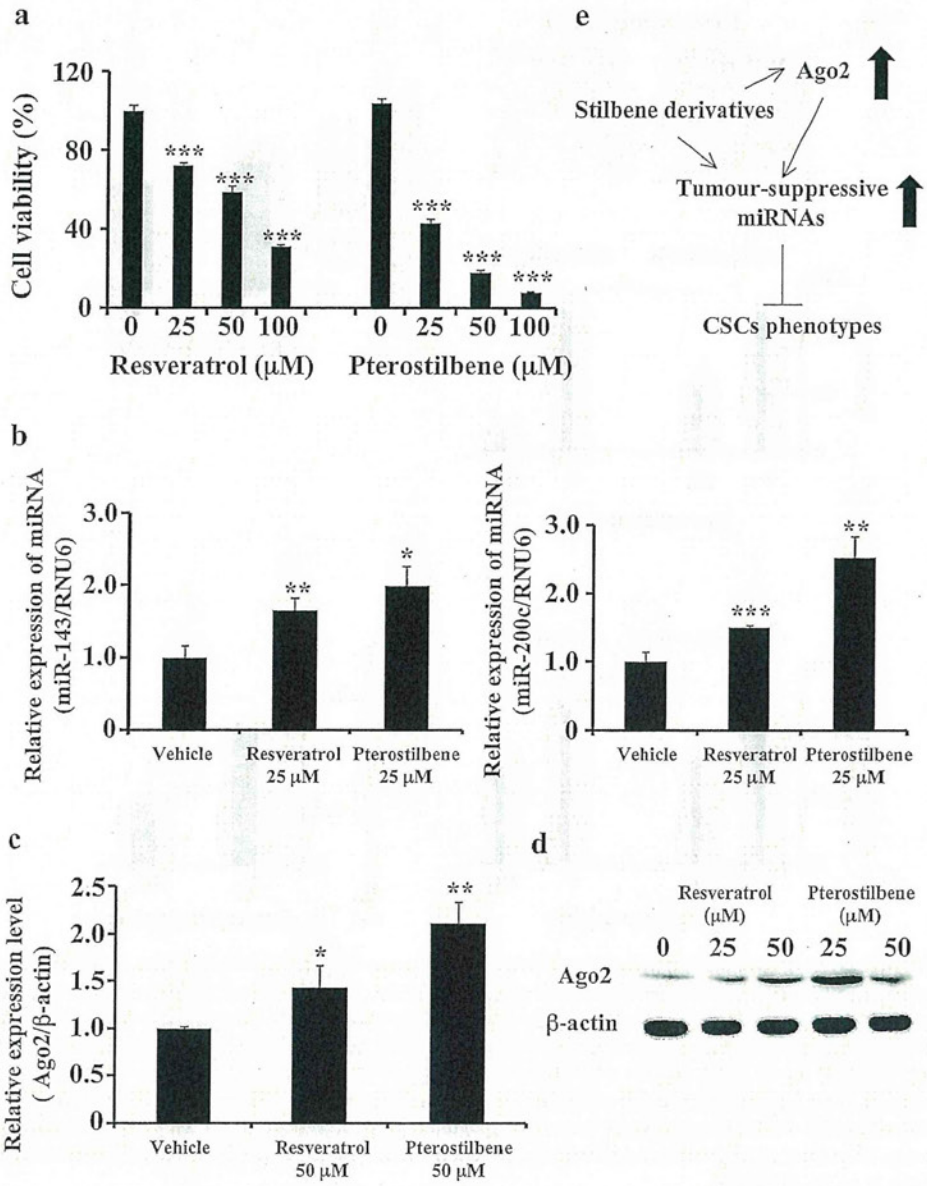

Figure 4 | Effects of pterostilbene on human breast cancer cells. (a) MDA-MB231-luc-D3H2LN cells were cultured in the presence or absence of resveratrol or pterostilbene at the indicated concentrations for 72 hours. Cell viability was measured using the MTS assay. The control wells were treated with DMSO. (b), (c) Expression levels of miR-143, miR-200c (b), and Ago2 (c) in MDA-MB231-luc-D3H2LN cells. The expression levels of the indicated miRNAs were examined in MDA-MB231-luc-D3H2LN cells 48 hours after treatment with pterostilbene. (d) MDA-MB231-luc-D3H2LN cells were treated with stilbenes for 72 hours, and Ago2 expression was detected by immunoblotting. Actin was used as a loading control. (e) Model of the regulation of tumour-suppressive miRNAs and Ago2 expression in the stilbene family (all data are shown as the mean ± s.e.m., *P<0.05, **P<0.01, ***P<0.001).

Medical Oncology, National Cancer Center Hospital of Japan. These cells were maintained in RPMI supplemented with 10% heat-inactivated FBS and antibiotic-antimycotic at 37°C in 5% CO_2. MCF10A cells, which were a spontaneously immortalized nontumorigenic epithelial cell line, (American Type Culture Collection) were maintained in an MEBM medium with 1% GA-1000, 50 μg/ml hydrocortisone, 1 μg/ml hEGF, 500 μg/ml insulin, and 4% BPE (Lonza) at 37°C in 5% CO_2.

Cell proliferation assay (MTS assay). Five thousand cells per well were seeded in 96-well plates. The following day, the cells were treated with resveratrol. After 3 days of culture, cell viability was measured using the Tetra Color One assay kit (Seikagaku Kohgyo) according to the instructions of the manufacturer. The absorbance at 450 nm was measured using Envision (Wallac).

Transwell invasion assay. Breast cancer cell invasion was assayed in 24-well Biocoat Matrigel invasion chambers (8 μm; Becton Dickinson) according to the manufacturer's protocol. Briefly, the cells were treated with resveratrol, and on the following day, 20,000 cells were plated in the upper chamber. The upper chamber contained resveratrol and the bottom chamber contained 10% FBS as a chemoattractant. Twenty-two hours later, the non-invasive cells were removed with a cotton swab. The cells that migrated through the membrane and stuck to the lower surface of the membrane were fixed with methanol and stained with Diff Quick staining. For quantification, the cells were counted under a microscope in four random fields. All assays were performed in triplicate. The data are expressed as the invasion percentage through the Matrigel matrix and membrane relative to migration through the control membrane according to the manufacturer's instructions.

Cell growth inhibition by cytotoxic agents and resveratrol. Breast cancer cells were plated as described above and allowed to attach overnight. The cultures were replenished with fresh medium containing 25 μM resveratrol for 24 hours and then exposed to 2.5 nM of the chemotherapeutic agent docetaxel for an additional 48 hours. Thus, for a single-agent treatment, the cells were exposed to resveratrol or docetaxel for 72 hours. The effect of resveratrol pretreatment on cell viability was examined by the MTS assay method.

Cell sorting and flow cytometric analysis. MDA-MB-231-luc-D3H2LN cells were treated with resveratrol. After culturing for 3 days, MDA-MB-231-luc-D3H2LN cells were suspended in their culture medium and subjected to a JSAN cell sorter (Bay Bioscience). At least one million cells were pelleted by centrifugation at 180 x *g* for 5 minutes at 4°C, resuspended in a 5-μL mixture of a monoclonal mouse anti-human CD44-FITC antibody (Becton Dickinson, clone L178) and a monoclonal mouse anti-human CD24-APC antibody (Biolegend, clone ML5), and incubated for 30 minutes at 4°C. Three independent experiments were performed.

Mammosphere assay. The CD44+/CD24− fraction from MDA-MB-231-luc-D3H2LN cells were resuspended in 1 : 1 DMEM/F12 (Invitrogen) basal medium freshly supplemented with 20 ng/mL human basic fibroblast growth factor (Invitrogen), 20 ng/mL epidermal growth factor (Invitrogen), 10 μg/mL heparin (Sigma-Aldrich), and 1 : 50 B27 supplement without vitamin A (Sigma-Aldrich) and seeded in 10-cm Ultra-Low Attachment Surface plates (Corning) at a density of 5000 cells. Ten days later, the plates were analysed for mammosphere formation.

Tumourigenicity assays in SCID hairless outbred mice. Six-week-old female SCID hairless outbred (SHO) mice were subcutaneously injected with 200 MDA-MB231-luc-D3H2LN cells in 25 μL of PBS and 25 μL of matrigel (n = 5). The mice were then treated with resveratrol (25 mg/kg/day) or ethanol (control) by intraperitoneal injection every day for 8 days. The tumour growth was monitored by injecting luciferin in the mice followed by measuring bioluminescence using an IVIS imaging system. The data were analysed using the LIVINGIMAGE 2.50 software (Xenogen). Six-week-old female SCID Hairless Outbred (SHO) mice were subcutaneously injected with 2000 MDA-MB231-luc-D3H2LN cells in 25 μL of PBS and 25 μL of Matrigel (n = 5). The mice were then treated with resveratrol (25 mg/kg) by intraperitoneal injection (IP) every day for 2 weeks and then with docetaxel (20 mg/kg) by intraperitoneal injection (IP) once per week for 2 weeks. The normalised fold changes (day 22 or day 29/day 15) of bioluminescence emitted from the whole body of the mice are shown. All experimental protocols involving animals were approved by the the Institute for Laboratory Animal Research, National Cancer Center Research Institute.

Isolation of microRNAs. Total RNAs were extracted from cultured cells using the QIAzol and miRNeasy Mini Kit (Qiagen) according to the manufacturer's protocol.

Quantitative Real-Time PCR (qRT-PCR). The qRT-PCR method has been previously described[38]. PCR was performed in 96-well plates using the 7300 Real-Time PCR System (Applied Biosystems). All reactions were performed in triplicate. All of the TaqMan microRNA assays were purchased from Applied Biosystems. hRNU6 was used as an invariant control. SYBR Green I qRT-PCR was performed, and the β-actin housekeeping gene was used to normalise the variation in the cDNA levels. The following pairs of primers were used for gene amplification: for pri-miR-16, 5′-GCAATTACAGTATTTTAAGAGATGAT-3′ (forward) and 5′- CAT-ACTCTACAGTTGTGTTTTAATGT-3′ (reverse); for pri-miR-141-200c, 5′-TGAGCTTGGGACTGCAGAG-3′ (forward) and 5′-CTGAGCCACCTTCCCC-TAC-3′ (reverse); for pri-miR-143, 5′-CAAGGTTTGGTCCTGGGTGCTCAAA-3′ (forward) and 5′-TGGTGGCCTGTGGCGGGACTCCAA-3′ (reverse); for ZEB1, 5′-AAGAATTCACAGTGGAGAGAAGCCA-3′ (forward) and 5′-CGTTTCTTGC-AGTTTGGGCATT-3′ (reverse); for E-cadherin, 5′-GTCCTGGGCAG-ACTGAATTT-3′ (forward) and 5′-GACCAAGAAATGGATCTGTGG-3′ (reverse); and for β-actin, 5′-GGCACCACCATGTACCCTG-3′ (forward) and 5′-CACGG-AGTACTTGCGCTCAG-3′ (reverse)[39].

Quantification of the Ago2 mRNA half-life. MDA-MB231-luc-D3H2LN cells were incubated with 5,6-dichlorobenzimidazole riboside (50 μM), which is an inhibitor of mRNA synthesis. The cells were then treated with 50 μM resveratrol and harvested at the indicated time points. Total cellular RNA was isolated using the RNeasy Mini kit (Qiagen). qRT-PCR analysis of Ago2 mRNA at each time point was performed as described above. The fold-change in the Ago2 mRNA abundance at each time point was determined by the following equation:

Fold change = $2^{-\Delta CT}$, where ΔCT = (CT, Ago2) target - (CT, Ago2) 0 h.

Transient transfection assays. The plasmid transfections were performed using Lipofectamine LTX (Invitrogen). The cell numbers and amount of plasmids for each transfection were determined according to the manufacturer's protocol. The transfection of siRNA and miRNA inhibitors was accomplished using the DharmaFECT transfection reagent (Thermo Scientific) according to the manufacturer's protocol.

Luciferase reporter assay. Cells were seeded in 96-well plates at 3000 cells per well the day before transfection. A total of 500 ng of Ago2 vector, 10 nM siRNA against luciferase and the AllStars negative control were added to each well. The cells were collected 1, 3, or 5 days after transfection and analysed using the Bright-Glo Luciferase Reporter Assay System (Promega).

Immunoblot analysis. SDS-PAGE gels were calibrated using Precision Plus protein standards (161-0375) (Bio-Rad), and anti-Ago2 (1 : 200) and anti-actin (1 : 1,000) were used as the primary antibodies. The dilution ratio of each antibody is indicated in parentheses. A peroxidase-labelled anti-mouse secondary antibody was used at a dilution of 1 : 10,000. Bound antibodies were visualised by chemiluminescence using the ECL Plus Western blotting detection system (RPN2132) (GE HealthCare), and luminescent images were analysed using a LuminoImager (LAS-3000; Fuji Film Inc.).

Quantification of Ago2 protein half-life. MDA-MB-231-luc-D3H2LN cells at 80% confluency were treated with 30 μg/ml cycloheximide (Sigma-Aldrich). The cells were then treated with 50 μM resveratrol and harvested at the indicated time points. The effect of resveratrol on Ago2 stability was examined by immunoblotting as reported above.

Statistical analysis. The data presented in bar graphs are the means ± s.e.m. of at least three independent experiments. Statistical analyses were performed using the Student's t-test.

1. Hartwell, J. L. & Schrecker, A. W. Components of Podophyllin. V. The Constitution of Podophyllotoxin1. *J Am Chem Soc* **73**, 2909–2916 (1951).
2. Baur, J. A. & Sinclair, D. A. Therapeutic potential of resveratrol: the in vivo evidence. *Nat Rev Drug Discov* **5**, 493–506 (2006).
3. Renaud, S. & de Lorgeril, M. Wine, alcohol, platelets, and the French paradox for coronary heart disease. *Lancet* **339**, 1523–1526 (1992).
4. Jang, M. *et al.* Cancer chemopreventive activity of resveratrol, a natural product derived from grapes. *Science* **275**, 218–220 (1997).
5. Fremont, L. Biological effects of resveratrol. *Life Sci* **66**, 663–673 (2000).
6. Hammell, C. M., Lubin, I., Boag, P. R., Blackwell, T. K. & Ambros, V. nhl-2 Modulates microRNA activity in Caenorhabditis elegans. *Cell* **136**, 926–938 (2009).
7. Stefani, G. & Slack, F. J. Small non-coding RNAs in animal development. *Nat Rev Mol Cell Biol* **9**, 219–230 (2008).
8. Kong, D. *et al.* miR-200 regulates PDGF-D-mediated epithelial-mesenchymal transition, adhesion, and invasion of prostate cancer cells. *Stem Cells* **27**, 1712–1721 (2009).
9. Zhao, J. J. *et al.* MicroRNA-221/222 negatively regulates estrogen receptor alpha and is associated with tamoxifen resistance in breast cancer. *J Biol Chem* **283**, 31079–31086 (2008).
10. Takeshita, F. *et al.* Systemic delivery of synthetic microRNA-16 inhibits the growth of metastatic prostate tumors via downregulation of multiple cell-cycle genes. *Mol Ther* **18**, 181–187 (2010).
11. Melkamu, T., Zhang, X., Tan, J., Zeng, Y. & Kassie, F. Alteration of microRNA expression in vinyl carbamate-induced mouse lung tumors and modulation by the chemopreventive agent indole-3-carbinol. *Carcinogenesis* **31**, 252–258 (2010).
12. Tsang, W. P. & Kwok, T. T. Epigallocatechin gallate up-regulation of miR-16 and induction of apoptosis in human cancer cells. *J Nutr Biochem* **21**, 140–146 (2010).
13. Li, Y. *et al.* Up-regulation of miR-200 and let-7 by natural agents leads to the reversal of epithelial-to-mesenchymal transition in gemcitabine-resistant pancreatic cancer cells. *Cancer Res* **69**, 6704–6712 (2009).
14. Sun, M. *et al.* Curcumin (diferuloylmethane) alters the expression profiles of microRNAs in human pancreatic cancer cells. *Mol Cancer Ther* **7**, 464–473 (2008).
15. Lee, H. P. *et al.* Dietary effects on breast-cancer risk in Singapore. *Lancet* **337**, 1197–1200 (1991).
16. Croce, C. M. Causes and consequences of microRNA dysregulation in cancer. *Nat Rev Genet* **10**, 704–714 (2009).
17. Gaur, A. *et al.* Characterization of microRNA expression levels and their biological correlates in human cancer cell lines. *Cancer Res* **67**, 2456–2468 (2007).
18. Al-Hajj, M., Wicha, M. S., Benito-Hernandez, A., Morrison, S. J. & Clarke, M. F. Prospective identification of tumorigenic breast cancer cells. *Proc Natl Acad Sci U S A* **100**, 3983–3988 (2003).
19. Al-Hajj, M. Cancer stem cells and oncology therapeutics. *Curr Opin Oncol* **19**, 61–64 (2007).
20. Al-Hajj, M., Becker, M. W., Wicha, M., Weissman, I. & Clarke, M. F. Therapeutic implications of cancer stem cells. *Curr Opin Genet Dev* **14**, 43–47 (2004).
21. Iorio, M. V. *et al.* MicroRNA gene expression deregulation in human breast cancer. *Cancer Res* **65**, 7065–7070 (2005).
22. Burk, U. *et al.* A reciprocal repression between ZEB1 and members of the miR-200 family promotes EMT and invasion in cancer cells. *EMBO Rep* **9**, 582–589 (2008).
23. Carmell, M. A. & Hannon, G. J. RNase III enzymes and the initiation of gene silencing. *Nat Struct Mol Biol* **11**, 214–218 (2004).
24. Kim, V. N. MicroRNA biogenesis: coordinated cropping and dicing. *Nat Rev Mol Cell Biol* **6**, 376–385 (2005).
25. Lingel, A., Simon, B., Izaurralde, E. & Sattler, M. Structure and nucleic-acid binding of the Drosophila Argonaute 2 PAZ domain. *Nature* **426**, 465–469 (2003).
26. Korpal, M., Lee, E. S., Hu, G. & Kang, Y. The miR-200 family inhibits epithelial-mesenchymal transition and cancer cell migration by direct targeting of E-cadherin transcriptional repressors ZEB1 and ZEB2. *J Biol Chem* **283**, 14910–14914 (2008).
27. Xu, B. *et al.* miR-143 decreases prostate cancer cells proliferation and migration and enhances their sensitivity to docetaxel through suppression of KRAS. *Mol Cell Biochem* **350**, 207–213 (2011).
28. Burk, U. *et al.* A reciprocal repression between ZEB1 and members of the miR-200 family promotes EMT and invasion in cancer cells. *Embo Reports* **9**, 582–589 (2008).

29. Rimando, A. M. *et al.* Cancer chemopreventive and antioxidant activities of pterostilbene, a naturally occurring analogue of resveratrol. *J Agric Food Chem* **50**, 3453–3457 (2002).
30. Stivala, L. A. *et al.* Specific structural determinants are responsible for the antioxidant activity and the cell cycle effects of resveratrol. *J Biol Chem* **276**, 22586–22594 (2001).
31. Shimono, Y. *et al.* Downregulation of miRNA-200c links breast cancer stem cells with normal stem cells. *Cell* **138**, 592–603 (2009).
32. O'Carroll, D. *et al.* A Slicer-independent role for Argonaute 2 in hematopoiesis and the microRNA pathway. *Genes Dev* **21**, 1999–2004 (2007).
33. Kapetanovic, I. M., Muzzio, M., Huang, Z., Thompson, T. N. & McCormick, D. L. Pharmacokinetics, oral bioavailability, and metabolic profile of resveratrol and its dimethylether analog, pterostilbene, in rats. *Cancer Chemother Pharmacol* (2010).
34. Chiou, Y. S. *et al.* Pterostilbene is more potent than resveratrol in preventing azoxymethane (AOM)-induced colon tumorigenesis via activation of the NF-E2-related factor 2 (Nrf2)-mediated antioxidant signaling pathway. *J Agric Food Chem* **59**, 2725–2733 (2011).
35. Chang, T. C. *et al.* Transactivation of miR-34a by p53 broadly influences gene expression and promotes apoptosis. *Mol Cell* **26**, 745–752 (2007).
36. Dhar, S., Hicks, C. & Levenson, A. S. Resveratrol and prostate cancer: Promising role for microRNAs. *Mol Nutr Food Res* **55**, 1219–1229 (2011).
37. Meister, G. *et al.* Human Argonaute2 mediates RNA cleavage targeted by miRNAs and siRNAs. *Mol Cell* **15**, 185–197 (2004).
38. Mitchell, P. S. *et al.* Circulating microRNAs as stable blood-based markers for cancer detection. *Proc Natl Acad Sci U S A* **105**, 10513–10518 (2008).
39. Suzuki, H. I. *et al.* Modulation of microRNA processing by p53. *Nature* **460**, 529–533 (2009).

Acknowledgements

This work was supported in part by a Grant-in-Aid for the Third-Term Comprehensive 10-Year Strategy for Cancer Control, a Grant-in-Aid for Scientific Research on Priority Areas Cancer from the Ministry of Education, Culture, Sports, Science and Technology, the National Cancer Center Research and Development Fund, the Program for Promotion of Fundamental Studies in Health Sciences of the National Institute of Biomedical Innovation (NiBio), Project for Development of Innovative Research on Cancer Therapeutics, and the Japan Society for the Promotion of Science (JSPS) through the "Funding Program for World-Leading Innovative R&D on Science and Technology (FIRST Program)" initiated by the Council for Science and Technology Policy (CSTP). We thank Ayako Inoue for excellent technical assistance. We thank Dr.Izuho Hatada for providing the information about Ago2 promoter region.

Author contributions

TO supervised the project. KH performed a significant amount of the experimental work. TO, KH, NK, and YY wrote the manuscript and prepared the figures and tables. *In vivo* experiments were carried out by KH, NK, YY, RT, and FT.

Additional information

Supplementary information accompanies this paper at http://www.nature.com/scientificreports

Competing financial interests: The authors declare no competing financial interests.

How to cite this article: Hagiwara, K. *et al.* Stilbene derivatives promote Ago2-dependent tumour-suppressive microRNA activity. *Sci. Rep.* **2**, 314; DOI:10.1038/srep00314 (2012).

OPEN ACCESS Freely available online

PLOS | ONE

Efficacy of a Novel Class of RNA Interference Therapeutic Agents

Tomohiro Hamasaki[1☯], Hiroshi Suzuki[1☯], Hisao Shirohzu[1☯], Takahiro Matsumoto[1,2], Corina N. D'Alessandro-Gabazza[2,3], Paloma Gil-Bernabe[2], Daniel Boveda-Ruiz[2], Masahiro Naito[3], Tetsu Kobayashi[3], Masaaki Toda[2], Takayuki Mizutani[1,5], Osamu Taguchi[3], John Morser[7], Yutaka Eguchi[6], Masahiko Kuroda[5], Takahiro Ochiya[4], Hirotake Hayashi[1], Esteban C. Gabazza[1,2*], Tadaaki Ohgi[1*]

1 BONAC Corporation, BIO Factory 4F, Aikawa, Kurume, Fukuoka, Japan, **2** Department of Immunology, Mie University Graduate School of Medicine, Mie, Japan, **3** Department of Pulmonary and Critical Care Medicine, Mie University Graduate School of Medicine, Mie, Japan, **4** National Cancer Center Research Institute, Tokyo, Japan, **5** Department of Molecular Pathology, Tokyo Medical University, Tokyo, Japan, **6** Laboratory of Molecular Genetics, Department of Medical Genetics, Osaka University Graduate School of Medicine, Osaka, Japan, **7** Division of Hematology, Stanford University School of Medicine, Stanford, California, United States of America

Abstract

RNA interference (RNAi) is being widely used in functional gene research and is an important tool for drug discovery. However, canonical double-stranded short interfering RNAs are unstable and induce undesirable adverse effects, and thus there is no currently RNAi-based therapy in the clinic. We have developed a novel class of RNAi agents, and evaluated their effectiveness *in vitro* and in mouse models of acute lung injury (ALI) and pulmonary fibrosis. The novel class of RNAi agents (nkRNA®, PnkRNA™) were synthesized on solid phase as single-stranded RNAs that, following synthesis, self-anneal into a unique helical structure containing a central stem and two loops. They are resistant to degradation and suppress their target genes. nkRNA and PnkRNA directed against TGF-β1mRNA ameliorate outcomes and induce no off-target effects in three animal models of lung disease. The results of this study support the pathological relevance of TGF-β1 in lung diseases, and suggest the potential usefulness of these novel RNAi agents for therapeutic application.

Citation: Hamasaki T, Suzuki H, Shirohzu H, Matsumoto T, D'Alessandro-Gabazza CN, et al. (2012) Efficacy of a Novel Class of RNA Interference Therapeutic Agents. PLoS ONE 7(8): e42655. doi:10.1371/journal.pone.0042655

Editor: Xiaolin Zi, University of California Irvine, United States of America

Received April 2, 2012; **Accepted** July 10, 2012; **Published** August 15, 2012

Funding: This work was supported in part by Grant-in-Aid from the Ministry of Education, Culture, Sports, Science, and Technology of Japan, and the Center of Excellence Grant from Mie University. No additional external funding received for this study. The funders were not involved in study design, data analysis, decision to publish, or preparation of the manuscript.

Competing Interests: TH, H. Suzuki, H. Shirohzu, T. Matsumoto and T. Mizutani are employees of BONAC Corporation. ECG, HH and T. Ohgi are members of the Board of Directors of BONAC Corporation. YE, MK, T. Ochiya, and JM are members of the Advisory Board of BONAC Corportation. Recently, the patent on nkRNA (WPO Patent WO/2012/005368A1) and PnkRNA (WPO Patent WO/2012/017919A1) became public, and in these patents, the names of HH, H. Shirohzu, TH, H. Suzuki are included. ECG has a pending patent (Patent 2011-237166) on the human TGF-beta1 transgenic mouse. The other authors have no conflict of interest. The products described above have not been as yet marketed. There are no further patents, products in development or marketed products to declare. This does not alter the authors' adherence to all the PLoS ONE policies on sharing data and materials, as detailed online in the guide for authors.

* E-mail: ohgi@bonac.co.jp (T. Ohgi); gabazza@doc.medic.mie-u.ac.jp (ECG)

☯ These authors contributed equally to this work.

Introduction

RNA interference (RNAi) is a natural mechanism for silencing gene expression that has been recently the focus of considerable attention for its potential application for the development of new drugs. During the process of RNAi, intracellularly introduced double-stranded (ds) RNA is cleaved into small interfering (si) RNA duplexes (19~21 base pairs) that are incorporated into a protein complex called the RNA-induced silencing complex (RISC), which unwinds the two siRNA strands, retaining one strand to allow the recognition and sequence-specific degradation of mRNA [1]. RNAi-based therapy may provide several advantages over conventional therapeutic approaches using small molecules and monoclonal antibodies [2]. Unlike traditional pharmaceutical drugs, RNAi therapeutic agents can inhibit all classes of gene targets with high selectivity and potency, can provide personalized therapy, can be easily synthesized and the steps of lead identification and optimization are rapid [3,4]. The proof-of-concept regarding the therapeutic applicability of RNAi was given by several *in vivo* studies performed in animal models of human disease. Inhibition of the expression of targeted genes and therapeutic efficacy have been successfully achieved with either local or systemic administration of siRNA in experimental animal models with diseases in the eyes, nervous system, viral infection, kidneys, liver, lungs or intestines. At present, there are more than ten RNAi-based drugs in clinical development [3].

Since its discovery a decade ago, RNAi has been widely used for functional gene studies in biomedical research and, currently, many efforts are being dedicated to harnessing their desirable properties for the development of new therapeutic drugs [5]. However, previous investigations made clear the existence of several obstacles needed to be overcome before their routine application in the clinic. Although siRNAs are more stable than ssRNAs, they are promptly degraded by nucleases when they are administered systemically [1]. The half-life of naked siRNAs is very short because they are rapidly degraded by nucleases from the serum and/or extracellular fluids [6]. Chemical modifications at specific positions have been shown to improve stability but they

may attenuate the suppressive activity of siRNAs [7]. The cost of large-scale production is another hurdle to the clinical application of chemically modified or unmodified siRNA agents [8]. Moreover, the systemic administration of naked or modified siRNAs may induce undesirable off-target effects by activating the innate immune system via TLR-dependent or independent mechanisms leading to increased secretion of inflammatory cytokines (IFN-α, IFN-β) [9]. Appearance of these undesirable events has been reported to be sequence- and cell-type-dependent [10,11]; many RNAi-based drugs have been withdrawn from clinical trials at early phase because the appearance of flu-like symptoms typical of an immune response [12]. Therefore, to achieve the ultimate goal of RNAi therapy, safety, effectiveness and delivery systems will need to be improved.

Pulmonary fibrosis is a chronic intractable disease and currently there are more than 5 million patients worldwide [13]. Transforming growth factor (TGF)-β1. plays critical roles in the pathogenesis of the disease by stimulating the proliferation of fibroblasts, by stimulating the secretion of extracellular matrix components and the recruitment and differentiation of myofibroblasts [14]. Several studies have also shown that TGF-β1 is implicated in the pathogenesis of acute lung injury (ALI) or acute respiratory distress syndrome (ARDS), which is another devastating disease with an overall mortality rate of 30~40% [15]. TGF-β1 can directly increase the permeability of both alveolar epithelial cells and pulmonary artery endothelial cells, and can decrease the function of ion channels.

In the current study, to overcome some of the drawbacks faced by current siRNA-based therapy, we developed a novel class of RNAi therapeutic agents. In addition, using this new technology, we prepared novel RNAi agents directed against TGF-β1 and their inhibitory activity was compared to canonical siRNA using *in vitro* assays and animal models of ALI and pulmonary fibrosis.

Results

Synthesis, structure and suppressive activity of novel classes of RNAi agents

The RNAi agents were synthesized as single-stranded RNAs on solid phase as described under material and method section. Proline diamide amidites were prepared and used to incorporate two proline derivatives into one RNA oligomer (**Figure 1**). The human GAPDH was selected as a representative RNAi target. A long (51 mer) single-stranded human GAPDH RNA oligonucleotide (**Table 1**) that contains two proline derivatives (P) was synthesized. We discovered that this RNA oligomer with proline derivatives self-anneals into a structure that has a central stem formed by the sense and antisense nucleotides, an unpaired site and a nucleotide loop at the left (5′-CC-P-GGCU-3′) and right (5′C-P-GAA-3′) ends containing a proline derivative (**Figure 2A**). This RNA was named PnkRNA.

A long (62 mer) single-stranded human GAPDH RNA oligonucleotide without the incorporation of proline derivatives was also synthesized. This single-stranded GAPDH RNA oligonucleotide was also found to self-anneal into a structure containing a central stem, a loop at the left and right ends and an unpaired site (**Figure 2B**). The central stem contains the sense and antisense nucleotides, the left loop is partially formed by a nucleotide cassette containing the sequence 5′-CUUCGGAA-3′, and the right loop is partially formed by a nucleotide cassette containing 5′-CCCCACACCGGCU-3′. RNAs with this structure were named nkRNAs.

Representative HPLC chromatogram and mass spectrum of the novel RNAi agents against human GAPDH, human and mouse TGF-β1 is described in **Figure S1**. The inhibitory effect of nkRNA and PnkRNA directed against human GAPDH was evaluated and compared with canonical human GAPDH siRNA. Similar to canonical siRNA, both nkRNA and PnkRNA showed strong suppressive activity of GAPDH expression in A549, HCT116 and HEK 293 cell lines (**Figure 3A, B, C**).

Inhibitory activity depends on position of unpaired sites

Both nkRNA and PnkRNA have a nicked site that is unpaired on their sense strands. We investigated if the location of that unpaired site is important by preparing self-annealed nucleic acids with unpaired sites at different positions on the sense strand of nkRNA directed against GAPDH mRNA (**Table S1; Figure 4A**). Their inhibitory activity was evaluated in the HCT 116 cells. Deletion of nucleotides from the left (positions −1, −2, −3) and right (positions −4, −5) cassettes of nkRNA and from the sense strand near the left (positions 1, 2, 3, 5) and right (positions 19, 20, 21) loops of nkRNA was associated with strong inhibitory activity (**Figure 4B**).

The *Tm* value of nkRNA was significantly correlated with its respective inhibitory activity, suggesting that the suppressive effect of nkRNA depends on the deleted position (**Figure 4C**). The *Tm* values for nkRNA and PnkRNA directed against human GAPDH were higher than the *Tm* for siRNA directed against human GAPDH (**Figure 4D**).

Weak suppressive activity of circular dumbbell-shaped RNA

A circular dumbbell-shaped RNA was previously reported to have stronger suppressive activity than canonical siRNA [16]. Dumbbell type nkRNA directed against human GAPDH was prepared to compare its inhibitory activity with the corresponding siRNA and nkRNA against human GAPDH. Treatment of RNA 5′ and 3′ ends with T4 polynucleotide kinase and T4 RNA ligase led to formation of a 50 base band on the PAGE that corresponds to the dumbbell-shaped RNA of GAPDH (**Figure 5A, B**). When the ligated band was eluted and tested for reduction of GAPDH mRNA in human HCT 116 cells, siRNA and nkRNA had a 10-fold stronger suppressive activity than the equivalent dumbbell RNA (**Figure 5C**).

In vitro activity of novel RNAi agents against TGF-β1

In order to test the novel RNAi agents against a gene involved in disease, nkRNA and PnkRNA directed against mouse TGF-β1 with deleted nucleotides at different positions were prepared (**Table S2**) and their suppressive effect was compared. TGF-β1 nkRNA and PnkRNA with deleted nucleotides at positions −2 and −3 showed stronger inhibitory activity than RNAi agents with deletion at positions 1 or 1+2 in Hepa 1–6 liver cell lines (**Figure S2A**). nkRNA and PnkRNA against mouse TGF-β1 also showed strong inhibitory activity in LA-4 lung epithelial cells (**Figure S2B**).

Digestion by Dicer

Cleavage of the two nucleotide overhangs at the 3′ end of a long double-stranded RNA by Dicer, a type III ribonuclease, leads to the intracellular release of functional 21 to 23 mer siRNAs [1]. To demonstrate that nkRNA and PnkRNA can be digested by Dicer, nkRNA dn1 and PnkRNA dn1 directed against mouse TGF-β1 (**Table S2**) were incubated with Dicer. Digestion of nkRNA and PnkRNA by Dicer led to the formation of 21~22 mer dsRNA (**Figure S3A, B, C** and **Table S3**), suggesting that the digestion